



Baird, A. F. (2019). Insights into fractures and fabric of shales from microseismicity. In *6th EAGE Shale Workshop*
<https://doi.org/10.3997/2214-4609.201900285>

Peer reviewed version

License (if available):
Unspecified

Link to published version (if available):
[10.3997/2214-4609.201900285](https://doi.org/10.3997/2214-4609.201900285)

[Link to publication record in Explore Bristol Research](#)
PDF-document

This is the accepted author manuscript (AAM). The final published version (version of record) is available online via EAGE at <https://doi.org/10.3997/2214-4609.201900285> . Please refer to any applicable terms of use of the publisher.

University of Bristol - Explore Bristol Research

General rights

This document is made available in accordance with publisher policies. Please cite only the published version using the reference above. Full terms of use are available:
<http://www.bristol.ac.uk/red/research-policy/pure/user-guides/ebr-terms/>

Introduction

Shales typically have very low matrix permeabilities due to their fine grain size, and thus form natural barriers to fluid flow unless fractures are present to provide fluid conduits. They are also often strongly anisotropic due to the high degree of preferred alignment of phyllosilicate minerals (Crystal Preferred Orientation, CPO) as well as bedding parallel laminations of organic material within the shale (Sayers, 2005). The presence of aligned fractures, either natural or induced by hydraulic stimulation, is another effective mechanism for generating seismic anisotropy. Here we show how observations of shear-wave splitting from microseismic data acquired from hydraulic fracture stimulation can be used to characterise the anisotropy of shales and infer properties of both fractures and rock fabric.

Methodology

One of the clearest indicators of seismic anisotropy is shear-wave splitting. When a shear wave generated by a microseismic event travels through an anisotropic medium it will split into two orthogonally polarised shear waves which propagate with different seismic velocities. The delay time between the arrival of the two shear waves is proportional to both the magnitude of the anisotropy and the ray path length. The polarisations of the fast and slow shear waves are controlled by the anisotropic symmetry of the medium. Therefore, by combining splitting measurements over a range of propagation azimuths and inclinations we can characterise the anisotropy of the medium. Microseismic datasets acquired from hydraulic fracture stimulations are often very large with tens of thousands of recorded events. To analyse these efficiently we use the semi-automated workflow of Wuestefeld et al. (2010) to estimate the shear-wave splitting and assess the robustness of the solutions.

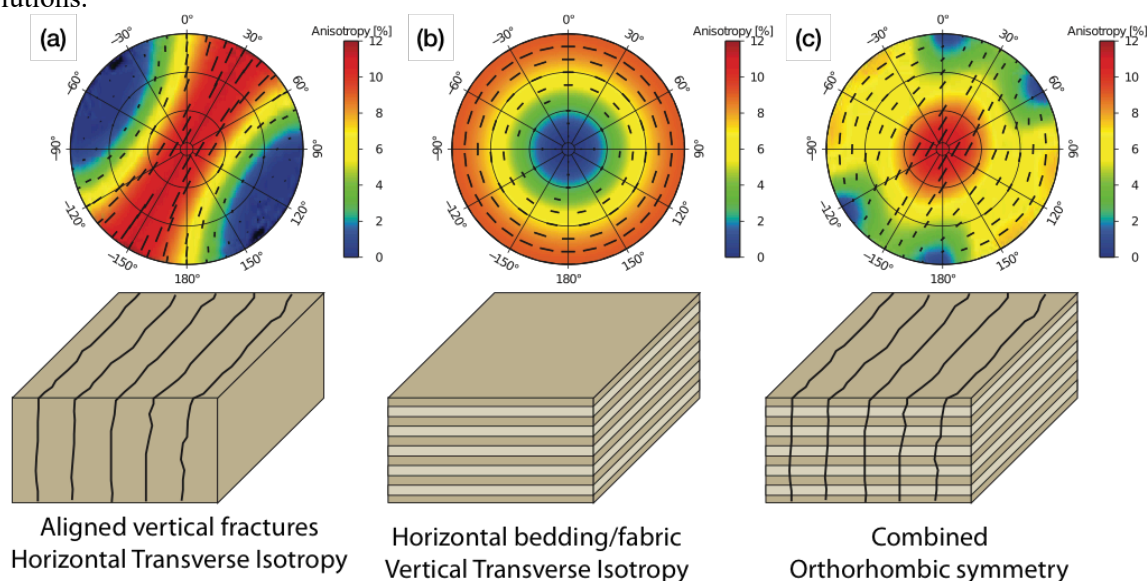


Figure 1 Synthetic upper hemisphere plots showing shear wave splitting magnitude (contours and tick lengths), and fast wave polarization (black tick orientations), for: (a) HTI anisotropy due to aligned vertical fractures; (b) VTI anisotropy due to horizontal layering/fabric; and (c) orthorhombic anisotropy due to vertical fractures in a horizontally layered medium. Position on the hemisphere indicates ray propagation direction (vertical in the centre, horizontal on the edges). Figure modified from Baird et al (2013).

Figure 1 illustrates the patterns of shear wave splitting expected due to (a) aligned vertical fractures, (b) horizontal bedding or fabric, and (c) combined vertical fractures in a horizontal fabric. Vertical fracture sets (Fig 1a) produce hexagonal anisotropy with a horizontal axis of symmetry (Horizontal Transverse Isotropy, HTI). Maximum splitting is observed for rays parallel to the fracture with magnitude proportional to fracture density and polarisation parallel to the fracture strike. A second order effect can sometimes be observed for rays propagating oblique to the fracture where splitting

parameters are sensitive to the ratio of the normal to tangential compliance of the fractures (Z_N/Z_T). Horizontal bedding or fabric (Fig 1b) produces anisotropy with a vertical rotational symmetry (Vertical Transverse Isotropy, VTI). VTI anisotropy is often described by the Thomsen (1986) parameters, ϵ , γ and δ . The most important parameter for shear wave splitting is γ which describes the fractional difference between the horizontal and vertical velocities for the horizontally polarised S wave (SH), and determines the amount of shear wave splitting for horizontally propagating rays. For rays with intermediate inclinations the ϵ and δ parameters also play a role since their relative magnitudes determine how the quasi-vertically polarised S wave (qSV) propagates. Finally, in most situations we would expect a contribution of both aligned vertical fractures embedded in a background with VTI fabric, which will produce an orthorhombic anisotropic symmetry (Fig. 1c). We use the approach of Verdon et al. (2009) to model and invert for both background VTI and vertical fracture properties.

Case studies

The first dataset comes from the stimulation of a tight gas sandstone with very little intrinsic anisotropy such that the observed anisotropy is dominated by HTI symmetry imposed by vertical fractures. Figure 2 shows a clear change in splitting parameters between the initial stage of the stimulation and subsequent stages, which implies a change in fracture parameters. The best fitting fracture model for Stage 1 suggests a strike of 30° (closely matching fracture orientations identified by downhole image logs) and a Z_N/Z_T ratio of 0.3. The best fitting model for later stages suggest a clockwise rotation of dominant fracture strike to 70° and an increase of Z_N/Z_T to 0.65. Based on this Baird et al. (2013) argue that pre-existing fractures are initially dominant, but in later stages new fractures are stimulated parallel to the direction of maximum horizontal compressive stress. The initial fractures have low Z_N/Z_T , which is indicative of fractures which are poorly connected or partially cemented, whereas later fractures are better connected to each other and to the porous matrix which would act to increase Z_N/Z_T .

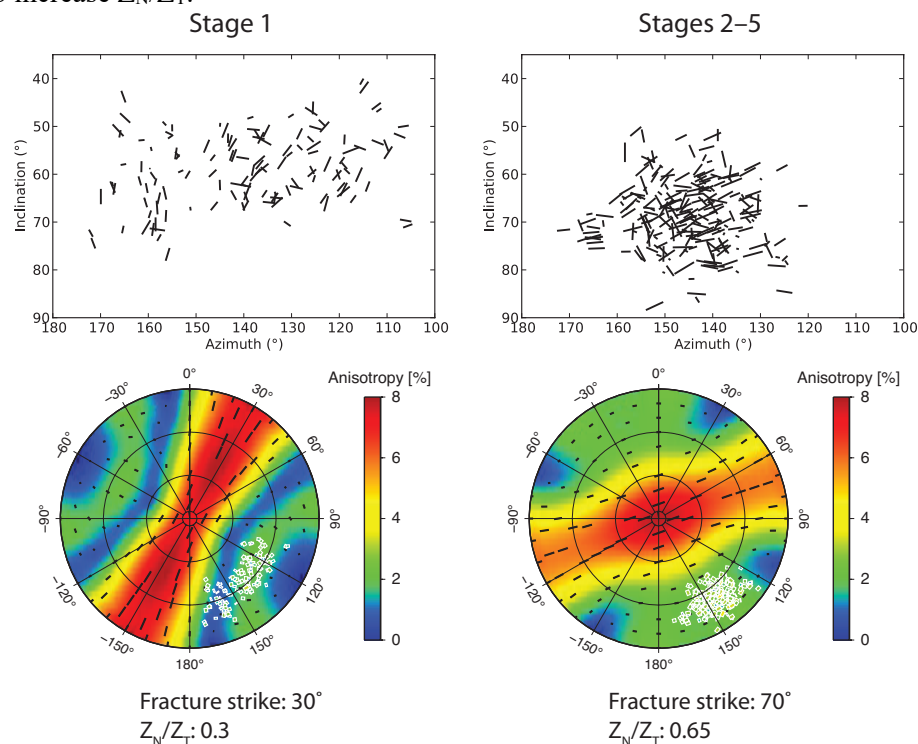


Figure 2 Top: Shear-wave splitting measurements presented in a cylindrical projection for stage 1 and subsequent stages 2-5 of a hydraulic fracture treatment. Tick orientations indicate the fast shear wave polarisation with vertical ticks indicating a quasi-vertical shear wave. Tick lengths are proportional to the percentage difference between the fast and slow shear velocities. Bottom plots show the best fitting models. Note that there is a rotation in the inferred fracture direction. Figure adapted from Baird et al. (2013).

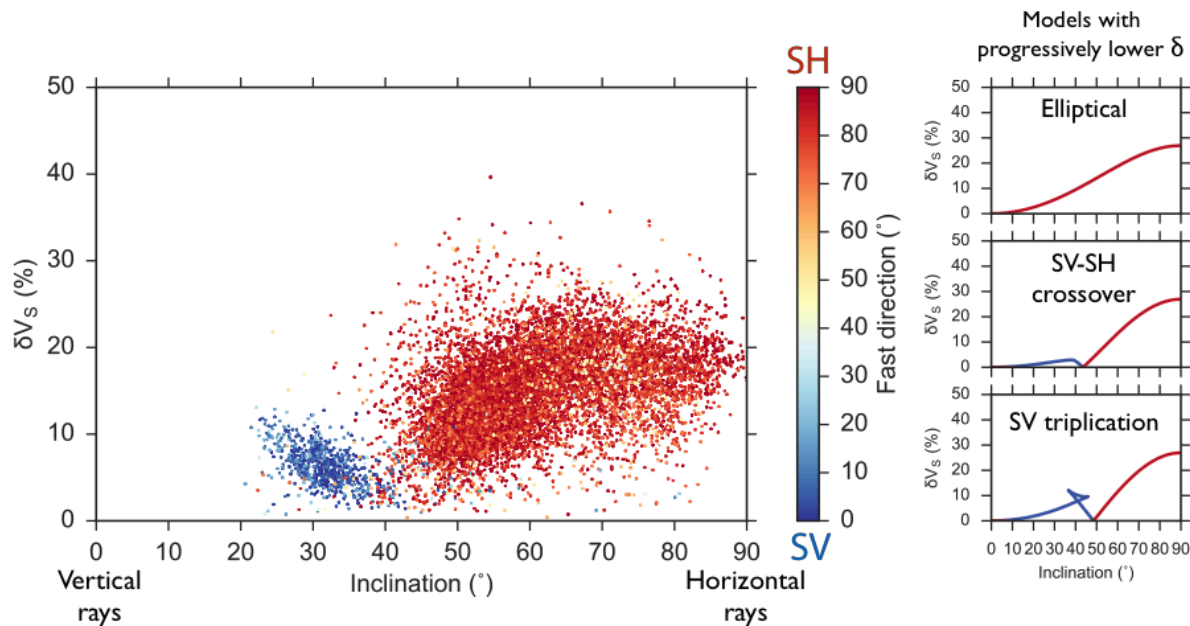


Figure 3 Left: Shear-wave splitting from the Horn River dataset as a function of ray inclination. Colour represents the polarization of the fast shear wave (qSV blue, SH red). Right: Predicted shear-wave splitting for VTI models with different values of δ . As δ is decreased qSV becomes faster than SH for steep inclinations and eventually produces a triplication. Figure adapted from Baird et al. (2017).

For more shaley reservoirs the preferred alignment of intrinsically anisotropic phyllosilicate minerals tends to produce a strong VTI fabric that dominates the anisotropy. This is the case for the second case study based on a large microseismic dataset acquired in the Horn River basin in Northeastern British Columbia. Approximately 92,000 events were detected on three downhole geophone arrays providing excellent ray coverage. Because of the array geometry the shear wave splitting primarily imaged the overlying Fort Simpson shale, which is very clay rich with strong intrinsic anisotropy. Figure 3 shows the variation in anisotropy with ray inclination from Baird et al (2017). For horizontal rays (90° inclination) the fast shear wave is horizontally polarised, however as inclination becomes more vertical qSV waves become faster. We can compare these splitting measurements to predictions made from Thomsen parameters. Based on sonic log information we have estimates of Thomsen's ϵ and γ , but not for δ , which is crucial for understanding how the qSV velocity (and thus shear wave splitting) varies with inclination. The right panel of figure 3 shows predicted splitting for an elliptical model ($\delta = \epsilon$), which predicts SH faster than qSV for all inclinations; and for models with progressively lower δ . As δ is decreased the qSV and SH wavefronts cross making qSV faster for steeper inclinations and better matching observations. If δ is lowered even further, the models predict that a triplication will occur in the SV phase. Based on this analysis, combined with observations of clear SV triplications in the recorded waveforms, Baird et al. (2017) provided a revised estimate of the Fort Simpson shale of $\epsilon = 0.33$, $\gamma = 0.46$, $\delta = 0.01$.

Discussion and Conclusions

Shear wave splitting from microseismic datasets provides an excellent method to characterise anisotropy of fractured shale reservoirs. We can then use these measurements to infer properties about the aligned fractures and sedimentary fabric. In the first dataset we see clear temporal variations in the magnitude and orientation of shear wave splitting, which must be the result of evolving properties in the fracture network. In the second dataset we show how shear wave splitting recorded over a large range of inclinations can be used to provide much better constraints on the VTI fabric of highly anisotropic shales.

One unresolved question is to what degree VTI anisotropy in shales can be explained by CPO and what effect horizontally aligned cracks and pores might contribute. Recent rock physics modelling and laboratory investigations suggests that the conversion of load bearing kerogen to oil and gas during thermal maturation of laminated organic rich shales effectively results in an increase in horizontally aligned pores, and thus an enhancement of the VTI anisotropy (Allan et al., 2016; Carcione & Avseth, 2015). In the Fort Simpson shale Baird et al. (2017), used modal proportions of minerals which a range of plausible textures to conclude that the anisotropy could be explained by CPO of clay minerals. However, the contribution of horizontal cracks could not be ruled out because the true orientation distribution functions of the minerals were unknown. Future work will involve using petrofabric analysis of samples from the shale to better estimate the intrinsic anisotropy due to CPO.

Acknowledgements

Funding for this work was provided by the sponsors of the Bristol University Microseismicity Projects (BUMPS), and by the Natural Sciences Research Council (NERC), as part of the SHAPE-UK project.

References

- Allan, A. M., Clark, A. C., Vanorio, T., Kanitpanyacharoen, W., and Wenk, H.-R. [2016] On the evolution of the elastic properties of organic-rich shale upon pyrolysis-induced thermal maturation. *Geophysics* **81** (3), D263–D281.
- Baird, A. F., Kendall, J.-M., Fisher, Q. J., Budge, J. [2017] The role of texture, cracks and fractures in highly anisotropic shales. *Journal of Geophysical Research: Solid Earth*, **122** (12).
- Baird, A. F., Kendall, J.-M., Verdon, J. P., Wuestefeld, A., Noble, T. E., Li Y., Dutko, M., Fisher, Q. J. [2013] Monitoring increases in fracture connectivity during hydraulic stimulations from temporal variations in shear-wave splitting polarization. *Geophysical Journal International*, **195** (2), 1120–1131.
- Carcione, J. M., and Avseth, P. [2015] Rock-physics templates for clay-rich source rocks. *Geophysics* **80** (5), D481–D500.
- Sayers, C., [2005] Seismic anisotropy of shales. *Geophysical Prospecting*, **53**, 667–676.
- Thomen, L. [1986] Weak elastic anisotropy. *Geophysics* **51** (10), 1954–1966.
- Verdon, J. P., Kendall, J.-M. and Wuestefeld, A. [2009] Imaging fractures and sedimentary fabrics using shear wave splitting measurements made on passive seismic data, *Geophysical Journal International*, **179**, 1245– 1254.
- Wuestefeld, A., Al-Harrasi, O., Verdon, J. P., Wookey, J. and Kendall, J.-M. [2010] Strategies for a fully automated passive microseismic anisotropy analysis, *Geophysical. Prospecting*, **58**, 755-773.